Journal of Alloys and Compounds, 194 (1993) 167–172
JALCOM 559

An investigation by EXAFS of the thermal dehydration and rehydration of cerium- and erbium-exchanged Y-zeolite

Frank J. Berry and José F. Marco
School of Chemistry, University of Birmingham, Edgbaston, Birmingham B15 2TT (UK)

Andrew T. Steel
Unilever Research, Port Sunlight Laboratory, Bebington, Wirral, Merseyside L63 3JW (UK)

(Received November 3, 1992)

Abstract

The changes in the local environments of cerium and erbium in rare-earth exchanged Y-zeolites which are induced by dehydration and rehydration processes have been investigated by extended X-ray absorption fine structure (EXAFS). The cerium L_3-edge EXAFS recorded from *ca.* 6 wt.% cerium-exchanged Y-zeolite show the hydrated cerium ion to be located in the large spaces in the supercages of the zeolite framework. Treatment *in vacuo* at 300 °C induces limited dehydration but the EXAFS study shows a closer approach of cerium to the zeolite framework. Washing of the material in ammonium chloride removes most of the cerium ions which are weakly held within the zeolite supercages but does not affect the ions located within the small cages. Treatment of the sample *in vacuo* at 300 °C induces the migration of most of the cerium into multiple site occupation of the small cages of the zeolite structure. Treatment in steam causes further changes in site occupancy and the migration of the cerium ions from the supercages in the zeolite framework.

The erbium L_3-edge EXAFS data recorded from *ca.* 8 wt.% erbium-exchanged Y-zeolite following identical treatments are essentially similar to those recorded from cerium-exchanged Y-zeolite.

1. Introduction

Lanthanide-ion exchanged Y-zeolites have been used for many years as hydrocarbon cracking catalysts in the petroleum industry [1–4]. The catalytic properties appear to depend on the nature, number, and location of the exchanged lanthanide cations [3] and the acidity of the zeolite framework [3]. Although infrared spectroscopy has been used successfully for the examination of the acidic hydroxyl groups in calcined zeolites [5] some difficulty remains in distinguishing between the hydroxyl groups which are attached to the lanthanide metal and those which are attached to the zeolite framework. Although X-ray diffraction, sometimes in conjunction with infrared spectroscopy, has been used to identify the different stages of dehydration of the hydrated lanthanide species at various temperatures [6–13] (and has also indicated the presence of adjacent lanthanide ions connected to bridging hydroxyl groups [6]) the partial occupation by the lanthanide ions of the exchange sites and the presence of coordinated water molecules has resulted in a less than unequivocal interpretation of the results. Furthermore, despite the success of recent neutron diffraction studies [14] of lanthanum-exchanged Y-zeolite which have described the hydrolysed lanthanum ions in terms of terminal rather than bridging hydroxyl groups, the exact description of the local environment of the rare-earth ions and the changes which are induced by thermal treatment remains the subject of considerable uncertainty.

The clarification of these matters is important since the presence of lanthanide ions is known to enhance the acidity and also preserve the structure of zeolites during their use as hydrocarbon cracking catalysts. Hence a description of the sites in the zeolite framework which are occupied by different lanthanide ions as a result of their different sizes and an understanding of how their local coordination changes as a result of dehydration and rehydration processes is crucial to an appreciation of their influence on the structural and catalytic chemistry of the materials. In this respect it is relevant to note the element specificity of extended X-ray absorption fine structure (EXAFS) and its superior sensitivity for elucidating the local coordination of the lanthanide ion as compared with that of conventional diffraction techniques. Given that EXAFS has recently been shown [15, 16] to be sensitive to the

0925-8388/93/$6.00

coordination of Eu^{3+} in hydrated A- and Y-zeolites, we have initiated an investigation by cerium and erbium L_3-edge EXAFS of the changes induced in the local coordination of cerium- and erbium-exchanged Y-zeolite as a result of dehydration and rehydration processes.

2. Experimental details

The lanthanide-exchanged Y-zeolites were prepared by the treatment of NH_4^+-exchanged zeolite with aqueous solutions of $ErCl_3 \cdot 6H_2O$ or $Ce(NO_3)_3 \cdot 6H_2O$ at 70 °C and pH 4.5 (30 min). The solids were washed, filtered, dried at 120 °C (12 h), and calcined at 250 °C (30 min). This exchange process was repeated twice after the low temperature drying treatment and once after calcination at 250 °C. The lanthanide-exchanged Y-zeolites were subsequently heated *in vacuo* at 300 °C (4 h), washed with 5% aqueous NH_4Cl solution and dried at 100 °C (4 h) before being heated at 300 °C (4 h) *in vacuo*. The freshly prepared materials were also treated in steam at 650 °C (30 min). Analytical data were obtained by atomic absorption spectroscopy and are collected in Table 1.

EXAFS measurements were performed at the Daresbury Synchrotron Radiation Source operating at an energy of 2.0 GeV and an average current of 200 mA at station 7.1 (cerium L_3-edge 5.729 keV, erbium L_3-edge 8.364 keV). The samples which had been treated in air were powdered and supported between strips of adhesive tape. The samples which had been prepared *in vacuo* were examined *in situ* using a glass cell with mylar windows. All data were recorded at room temperature. The raw data were background-subtracted and converted into k space. The data were weighted by k^3, where k is the photoelectron wavevector, to compensate for the diminishing amplitude of the EXAFS at high k. The data were fitted using the non-linear least squares minimisation programme [17] EXCURV 90 which calculates the theoretical EXAFS function using the fast curved wave theory [18]. In the case of the cerium-containing samples, the calculated phase shifts were tested on $Ce(NO_3)_3 \cdot 6H_2O$ and the results found to be in good agreement with the crystallographic data [19] (Table 1). However, the Fourier transform of the EXAFS data consistently recorded from this material showed a peak at 3.72 Å (Fig. 3[i]) which was best fitted to a shell of four oxygen atoms and was not present in the published crystallographic data. In the absence of more recent diffraction data we are unable to account for the origin of this feature in both the filtered and unfiltered EXAFS data. In the case of the erbium-containing samples the phase shifts were tested on $ErCl_3 \cdot 6H_2O$. (The EXAFS recorded from this compound and its Fourier transform are shown in Figs. 3[i] and 4[i] respectively.) The best fit parameters are contained in Table 2.

An inherent problem in EXAFS data analysis is the difficulty of determining coordination numbers to a high degree of accuracy. This is chiefly because a strong correlation exists between the coordination numbers of each shell and its associated Debye–Waller factor which is a measure of the thermal and/or static disorder of the atoms in the shell. During the initial analysis of the data approximate values for coordination numbers were obtained by allowing the occupancies and Debye–Waller factors to refine. The coordination numbers were then allowed to refine separately. The quality of the fit to the data was assessed by using statistical tests [20] and found to be significant at the 1% level.

TABLE 1. Analytical data determined by atomic absorption spectroscopy

Sample	Ce (wt.%)	Total volatile matter (wt.%)
Ce-exchanged Y-zeolite	5.9	21.0
vacuo, 300 °C	5.9	17.6
wash, NH_4Cl	5.2	23.1
Er-exchanged Y-zeolite	8.4	24.9
vacuo, 300 °C	8.4	14.8
wash, NH_4Cl	7.1	26.1

TABLE 2. Cerium–oxygen and erbium–oxygen distances (Å) in cerium(III) nitrate hexahydrate and erbium(III) chloride hexahydrate

	EXAFS	(XRD) [19]
Ce–O in	2.54	2.53
$Ce(NO_3)_3 \cdot 6H_2O$	2.71	2.72
	3.72	–
Er–O in		
$Er(Cl_3) \cdot 6H_2O$	2.32	–

3. Results and discussion

The cerium L_3-edge EXAFS recorded from the cerium-exchanged Y-zeolites and their Fourier transforms are shown in Figs. 1 and 2 respectively. The best fit parameters are contained in Table 3.

The Fourier transform of the EXAFS recorded from the cerium exchanged Y-zeolite (Fig. 3[ii]) was characterised by a main peak at *ca.* 2.5 Å and several other peaks at longer distances. The best fit to the data was achieved by considering two contributions to the main peak: (i) four oxygen atoms at 2.50 Å and (ii) five oxygen atoms at 2.67 Å. The result is similar to that

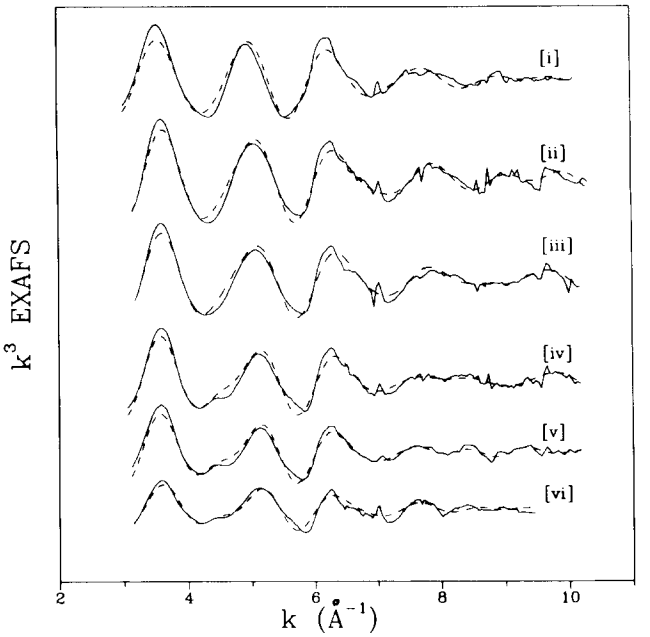

Fig. 1. Cerium L_3-edge EXAFS recorded from: [i] cerium (III) nitrate hexahydrate; [ii] cerium exchanged Y-zeolite and following sequential treatment; [iii] *in vacuo* at 300 °C (4 h); [iv] in ammonium chloride solution and dried at 120 °C (12 h); [v] *in vacuo* at 300 °C (4 h); [vi] steam at 650 °C (30 min). The experimental data are indicated by the solid line.

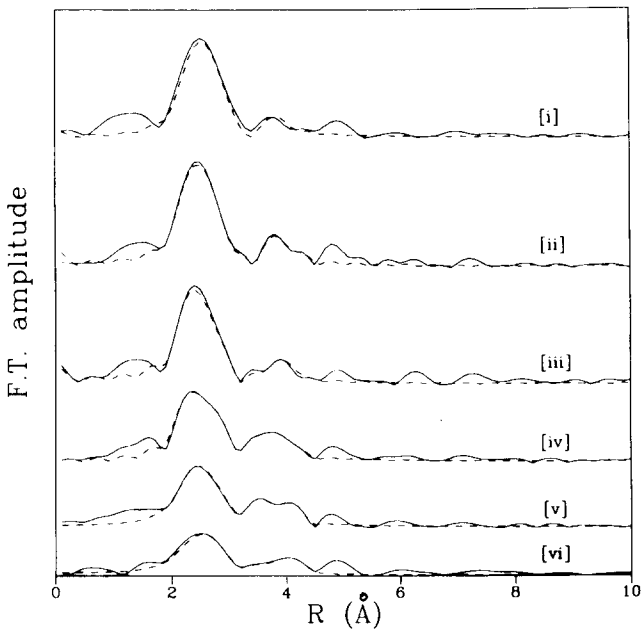

Fig. 2. Fourier transforms of EXAFS depicted in Fig. 1. The experimental data are indicated by the solid line.

recorded from cerium nitrate hexahydrate although the distances are shorter by *ca.* 0.04 Å. The second shell in the Fourier transform may be associated with back-scattering from silicon, aluminium and oxygen in the zeolite framework. The result suggests that cerium is located as a hydrated ion in the large spaces in the supercages of the zeolite framework although the existence of a Ce–Si distance of 4.02 Å (Table 3) indicates that cerium is partially bonded to oxygen atoms in the zeolite framework.

The data recorded from the material following heating *in vacuo* at 300 °C were similar (Figs. 1 and 2). The main differences were: (i) a reduction in the amplitude of the main peak in the Fourier transform by *ca.* 10% and which is reflected by the increase in the Debye–Waller factors of the two shells of oxygen atoms contributing to the peak (Table 3); (ii) the appearance of a closer shell of silicon atoms (Table 3). The appearance of a new shell of silicon atoms suggests that the cerium ions are more strongly bound to the zeolite framework and may indicate some migration into the smaller cages. The reduction in the total volatile matter content is consistent with some partial structural dealumination but can also be associated with the irreversible dehydration of cerium ions that have become bound to the framework such that their coordination requirements are satisfied by fewer mobile water molecules.

The EXAFS and Fourier transform recorded from the material washed in ammonium chloride (Figs. 1[iv] and 2[iv]) showed a decrease in the first cerium–oxygen shell amplitude by *ca.* 20% compared with that of the freshly prepared cerium-exchanged zeolite. The cerium content in the washed material was found to decrease by *ca.* 20% and we envisage this to correspond to the loss of loosely held fully hydrated cerium cations that are not located by the calcination treatment. This fraction would enjoy a well-ordered first coordination shell and the removal of these species is consistent with the loss of the first shell EXAFS amplitude. We envisage that the cerium ions in the large cages have a well-ordered coordination similar to that in hydrated Ce^{3+} cations which contributes significantly to the EXAFS. The removal of these species by washing in ammonium chloride leads to a reduction in EXAFS amplitude such that the EXAFS become dominated by the well-bound species which are apparently more disordered and spread over several bound sites. Taken together, the results indicate the existence of enhanced bonding interactions between cerium and the zeolite framework and thereby suggest that washing removes most of the cerium ions that are weakly held within the zeolite supercages but does not affect the cerium ions which are located within the smaller cages.

The data recorded from the ammonium chloride-washed cerium-exchanged zeolite heated *in vacuo* at 300 °C (Figs. 1 and 2[v]) showed a *ca.* 40% reduction in the amplitude of the main peak in the Fourier transform compared with that recorded from the freshly exchanged zeolite. This is reflected by the Debye–Waller factors associated with both cerium–oxygen distances. The splitting of the second shell demonstrates the

TABLE 3. Final fitting parameters obtained from cerium L_3-edge EXAFS data

Sample	Ce–O			Ce–Si		
	N	*R* (Å)	$2\sigma^2$ (Å^2)	*N*	*R* (Å)	$2\sigma^2$ (Å^2)
Exchanged	4	2.50	0.002	2	4.02	0.011
	5	2.67	0.002	–	–	–
	2	3.34	0.008	–	–	–
	4	3.65	0.006	–	–	–
Heated *in vacuo*	4	2.51	0.005	1	3.29	0.031
300 °C (4 h),	5	2.68	0.010	2	4.01	0.032
measured *in vacuo*	4	3.66	0.041	–	–	–
Washed with 5%	4	2.50	0.012	2	3.35	0.032
aqueous NH_4Cl and	5	2.69	0.015	2	4.06	0.040
dried at 120 °C (4 h)	4	3.66	0.032	–	–	–
Heated *in vacuo*	4	2.53	0.024	2	3.41	0.024
300 °C (4 h)	5	2.70	0.032	2	4.08	0.027
measured *in vacuo*	4	3.66	0.049	–	–	–
Steam treated	3	2.51	0.026	2	3.37	0.035
	3	2.67	0.022	2	4.03	0.025

enhanced importance of the shorter cerium–silicon distances. The results suggest that the heat treatment increases the disorder in the first shell and further enhances the binding of cerium to the zeolite framework. It is likely that this treatment induces the migration of most of the remaining hydrated cerium ions from the supercages into the smaller cages of the zeolite and the results are quite consistent with multiple site occupation. The observed cerium–oxygen distance of 2.51 Å is similar [19] to that between cerium and the oxygen atom of water in the compound $Ce(NO_3)_3 \cdot 6H_2O$. The result is compatible with the presence of some cerium in the S(I′) site inside the sodalite unit. In this situation the cerium ion would be bonded to three oxygen atoms of the six-membered ring and to some water molecules in the sodalite unit. The possible location of some cerium in the large spaces of the zeolite supercage cannot be discounted although it might be expected that most of these species would be removed during the washing process.

The Fourier transform of the EXAFS recorded from the steam treated sample (Fig. 2[vi]) showed a decrease in the amplitude of the main peak by *ca.* 60% compared with the freshly exchanged zeolite. The fitting of the first two shells around cerium with coordination numbers of 4 and 5 gave very high Debye–Waller factors. The best fit to the data was achieved by allowing the coordination numbers and the Debye–Waller factors to refine together to give a coordination number of 3 for the two shells. The results suggest that the steam treatment causes all the cerium ions to migrate into the smaller cages of the zeolite framework. The data are compatible with the occupation by cerium of the S(I′) sites such that each cerium ion is bonded to three oxygen atoms of the six-membered ring and to three water molecules. A similar result has been recorded from steam-treated lanthanum-exchanged Y-zeolites [8].

The erbium L_3-edge EXAFS recorded from erbium-exchanged Y-zeolite and their Fourier transforms are shown in Figs. 3 and 4 respectively. The best fit parameters are contained in Table 4.

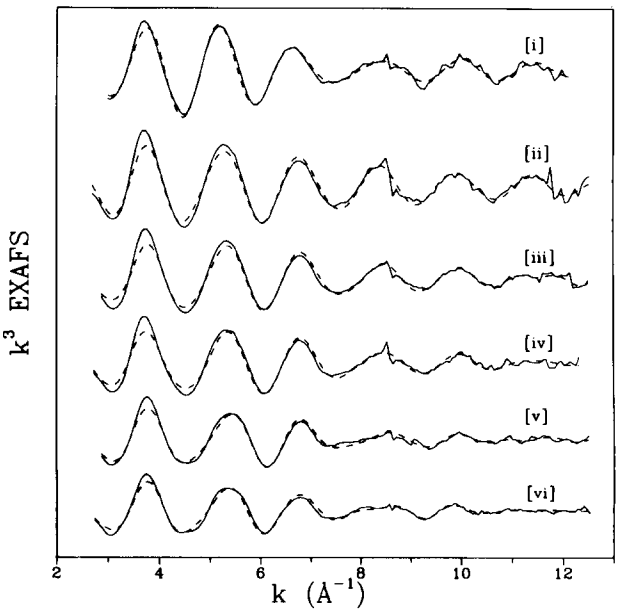

Fig. 3. Erbium L_3-edge EXAFS recorded from: [i] erbium (III) chloride hexahydrate; [ii] erbium exchanged Y-zeolite and following sequential treatment; [iii] *in vacuo* at 300 °C (4 h); [iv] in ammonium chloride solution and dried at 120 °C (12 h); [v] *in vacuo* at 300 °C (4 h); [vi] steam at 650 °C (30 min). The experimental data are indicated by the solid line.

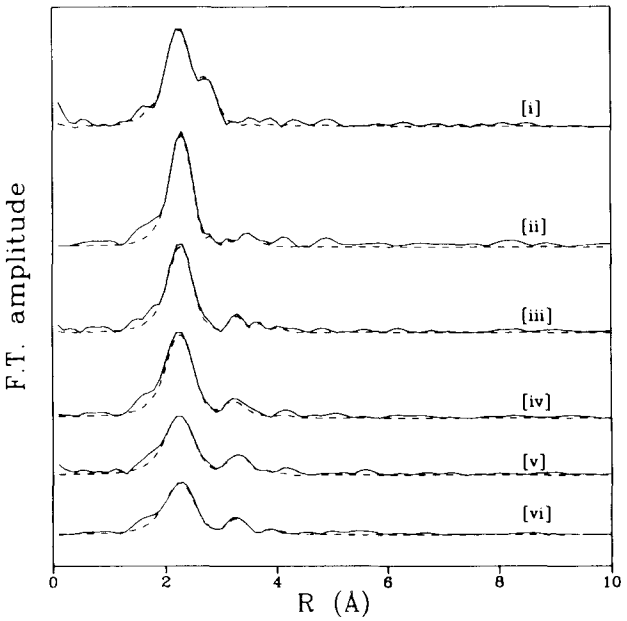

Fig. 4. Fourier transforms of EXAFS depicted in Fig. 3. The experimental data are indicated by the solid line.

The Fourier transform of the EXAFS (Fig. 4[ii]) showed a main peak corresponding to a shell of six oxygen atoms at 2.34 Å, together with smaller peaks corresponding to the presence of oxygen atoms at longer distances. The first oxygen coordination shell and associated Debye–Waller factors were similar to those recorded from the erbium chloride hexahydrate. The necessity to fit two cerium–oxygen distances to the first shell (as opposed to one erbium–oxygen distance) is indicative of a more symmetrical environment for the erbium-containing materials. The result is consistent with the location of hydrated erbium species within the larger spaces of the zeolite.

Analysis of the erbium-exchanged Y-zeolite following treatment *in vacuo* and washing in ammonium chloride gave data which showed similar trends to those identified in the cerium-exchanged zeolite. The Fourier transform of the EXAFS (Fig. 4[iii]) showed the amplitude of the main peak to decrease by *ca.* 20%. The smaller peaks at longer distances were best fitted to shells of silicon atoms. The results suggest that this treatment induces a closer approach of erbium to the zeolite framework as postulated for the cerium-exchanged zeolite (see above). This may involve partial bonding of erbium located in the supercages to the zeolite framework together with the migration of some erbium into the smaller cages of the zeolite.

The Fourier transform of the EXAFS recorded from the ammonium chloride-washed zeolite (Fig. 4[iv]) showed a decrease in the amplitude of the main peak by *ca.* 40% compared with the freshly exchanged zeolite. The results may, as in the case of the cerium-exchanged

TABLE 4. Final fitting parameters obtained from erbium L_3-edge EXAFS data

Sample	Ce–O			Ce–Si		
	N	*R* (Å)	$2\sigma^2$ (Å^2)	*N*	*R* (Å)	$2\sigma^2$ (Å^2)
Exchanged	6	2.34	0.013	–	–	–
	2	3.00	0.015	–	–	–
	2	3.18	0.003	–	–	–
	2	3.33	0.004	–	–	–
	2	3.45	0.011	–	–	–
Heated *in vacuo* 300 °C	6	2.33	0.018	1	3.22	0.014
(4 h), measured *in vacuo*	–	–	–	2	3.53	0.013
	–	–	–	2	3.70	0.009
	–	–	–	2	3.86	0.018
Washed with 5% aqueous	6	2.33	0.020	1	3.15	0.020
NH_4Cl and dried at	–	–	–	2	3.54	0.025
120 °C (4 h)	–	–	–	2	3.71	0.019
	–	–	–	2	3.89	0.025
Washed and heated	6	2.31	0.028	1	3.15	0.022
in vacuo 300 °C (4 h),	–	–	–	2	3.53	0.017
measured *in vacuo*	–	–	–	2	3.70	0.019
	–	–	–	2	3.85	0.031
Steam treated	6	2.34	0.030	1	3.17	0.024
	–	–	–	2	3.55	0.013
	–	–	–	2	3.73	0.009
	–	–	–	2	3.91	0.018

material when subjected to similar treatment (see above), indicate that the treatment removes erbium ions located within the zeolite supercages without affecting the erbium ions located within the smaller cages. The shortening of the first erbium–silicon distance by 0.07 Å suggests a stronger interaction of erbium with the zeolite framework.

The Fourier transform of the EXAFS recorded from the ammonium chloride-washed erbium exchanged zeolite following heating *in vacuo* at 300 °C (Fig. 4[v]) showed a decrease of about 50% in the amplitude of the first peak compared with the freshly exchanged material. The result is indicative of increased disorder arising from multiple site occupancy. The erbium–silicon distances remained essentially unchanged, indicating that many of the sites have similar second shell coordination.

The data recorded from the steam-treated sample (Fig. 3[vi] and 4[vi]) showed a decrease in amplitude of the first shell which is similar to that observed in the sample which had been washed and heated *in vacuo* at 300 °C. The interatomic distances were found to increase by *ca.* 0.02–0.03 Å. The results suggest that the balance of occupation of the various sites is altered by this treatment.

Taken together, the results show that thermal dehydration and rehydration of cerium- and erbium-exchanged zeolites results in changes in local coordination. These variations can be associated with changes in the balance of multiple-site occupancy which are similar in some respects to effects recently observed in some nickel-exchanged zeolites [21]. The observed consistency in the fitted distances reflects the similar coordination geometries of many of these sites.

Acknowledgments

We thank Ministerio de Educacion y Ciencia (Spain) for the award of a fellowship (JFM). We thank the S.E.R.C. for support.

References

1 C. N. Satterfield, *Heterogeneous Catalysis in Practice,* McGraw-Hill, New York, 1980, p. 174.
2 A. P. Bolton, in J. A. Rabo (ed.), *Zeolite Chemistry and Catalysis,* ACS Monograph 171, American Chemical Society, Washington DC, 1976, Chapter 1.
3 N. D. Spencer and G. A. Somorjai, *Rep. Prog. Phys., 46* (1983) 1.
4 A. P. Bolton, *J. Catal., 22* (1971) 9.
5 J. W. Ward, in J. A. Rabo (ed.), *Zeolite Chemistry and Catalysis,* ACS Monograph 171, American Chemical Society, Washington DC, 1976, Chapter 3.
6 J. V. Smith, J. M. Bennet and E. M. Flaningen, *Nature, 215* (1967) 241.
7 D. H. Olson, G. T. Kotkotailo and J. F. Charnell, *J. Colloid Interface Sci., 28* (1968) 305.
8 F. D. Hunter and J. Scherzer, *J. Catal., 20* (1971) 246.
9 J. Scherzer, J. L. Bass and F. D. Hunter, *J. Phys. Chem., 79* (1975) 1194.
10 J. Marti, J. A. Rubio, J. Soria and F. H. Cano, *An. Quim. Ser. A, 84* (1988) 68.
11 J. Marti, J. Soria and F. H. Cano, *J. Colloid Interface Sci., 67* (1978) 266.
12 D. H. Olson, G. T. Kokotailo and J. F. Charnell, *Nature, 215* (1967) 271.
13 P. Gallezot and B. Imelik, *J. Chem. Phys. Physiochem. Biol., 68* (1971) 37.
14 A. K. Cheetham, M. M. Eddy and J. M. Thomas, *J. Chem. Soc. Chem. Commun.* (1984) 1337.
15 G. D. Stucky, L. E. Iton, T. I. Morrison, G. K. Shenoy, S. Suib and R. P. Zerger, *J. Mol. Catal., 27* (1984) 71.
16 S. L. Suib, R. P. Zerger, G. D. Stucky, T. I. Morrison and G. K. Shenoy, *J. Chem. Phys., 80* (1984) 2203.
17 N. Binsted, S. Gurman and J. Campbell, Daresbury Laboratory EXCURV 90 Program.
18 S. J. Gurman, N. Binsted and I. Ross, *J. Phys. C., 17* (1984) 143.
19 N. Milinski, B. Ribar and M. Sataric, *Cryst. Str. Commun., 9* (1980) 473.
20 R. W. Joyner, K. J. Martin and A. Meehan, *J. Phys. C., 20* (1987) 4005.
21 E. Dooryhee, C. R. A. Catlow, J. W. Couves, P. J. Maddocks, J. M. Thomas, G. N. Greaves, A. T. Steel and R. T. Townsend, *J. Phys. Chem., 95* (1991) 4514.